Influence of Ni/Mn ratio on magnetostructural transformation and magnetocaloric effect in $Ni_{48-x}Co_2Mn_{38+x}Sn_{12}$ ($x = 0$, 1.0, 1.5, 2.0, and 2.5) ferromagnetic shape memory alloys*

Ishfaq Ahmad Shah[1], Najam ul Hassan[1], Abdur Rauf[2], Jun Liu(刘俊)[1], Yuanyuan Gong(龚元元)[1], Guizhou Xu(徐桂舟)[1], and Feng Xu(徐锋)[1,†]

[1] *Jiangsu Key Laboratory of Advanced Micro & Nano Materials and Technology, School of Materials Science and Engineering, Nanjing University of Science and Technology, Nanjing* 210094, *China*

[2] *Herbert Gleiter Institute of Nanoscience, Nanjing University of Science and Technology, Nanjing* 210094, *China*

(Received 27 April 2017; revised manuscript received 23 May 2017; published online 9 August 2017)

An investigation on the magnetostructural transformation and magnetocaloric properties of $Ni_{48-x}Co_2Mn_{38+x}Sn_{12}$ ($x = 0$, 1.0, 1.5, 2.0, and 2.5) ferromagnetic shape memory alloys is carried out. With the partial replacement of Ni by Mn in the $Ni_{48}Co_2Mn_{38}Sn_{12}$ alloy, the electron concentration decreases. As a result, the martensitic transformation temperature is decreased into the temperature window between the Curie-temperatures of austenite and martensite. Thus, the samples with $x = 1.5$ and 2.0 exhibit the magnetostructural transformation between the weak-magnetization martensite and ferromagnetic austenite at room temperature. The structural transformation can be induced not only by the temperature, but also by the magnetic field. Accompanied by the magnetic-field-induced magnetostructural transformation, a considerable magnetocaloric effect is observed. With the increase of x, the maximum entropy change decreases, but the effective magnetic cooling capacity increases.

Keywords: Ni–Co–Mn–Sn alloy, magnetostructural transformation, magnetocaloric effect, magnetic entropy change

PACS: 75.30.Sg **DOI:** 10.1088/1674-1056/26/9/097501

1. Introduction

Room-temperature magnetic refrigeration is an innovative cooling technology with the advantages of high efficiency, low cost, and environmental friendliness. In this technology, magnetic materials are used as the refrigerants. To maximize the cooling capacity of magnetic refrigeration at room temperature (RT), the magnetic refrigerants should exhibit a large magnetic entropy or temperature change under a magnetic field.[1–4] During the last decade, the large magnetocaloric effect (MCE) has been successively observed in magnetic alloys that experience a magnetic-field-induced first-order phase transition, including Gd–Si–Ge-based alloys,[5] $MnAs_{1-x}Sb_x$,[6] Mn–Fe–P–As,[7] La $(Fe_{1-x}Si_x)_{13}$,[8] and especially, Ni–Mn-based magnetic shape memory alloys.[9,10]

Rare-earth-free Ni–Mn-based magnetic shape memory alloys (Ni–Mn–X, X = Al, Ga, Sn, In and Sb) display a structural transformation between magnetic martensite and austenite. Various investigations on the structural, magnetic, and electrical properties of these alloys have been carried out.[11–17] It is found that the first-order magnetostructural transformation (MST) from the high-temperature austenite to the low-temperature martensite is accompanied by an obvious magnetization difference (ΔM) in some alloys with specific compositions. Due to the existence of ΔM, the MST can be driven by a magnetic field, and thus a large MCE can be achieved.[18–22]

Among Ni–Mn–X alloys, Ni–Mn–Sn attracts considerable attention due to its tunable MST, large MCE, and relatively low cost. From the application point of view, the designed material as a magnetic refrigerant should display the MCE and large effective refrigeration capacity (RC_{eff}) at RT. In this work, we select $Ni_{48}Co_2Mn_{38}Sn_{12}$ as the starting composition, which experiences a structural transformation above RT. By changing the Ni/Mn ratio, the structural transformation temperature (T_t) is decreased to RT. Meanwhile, the structural transformation is tuned into the Curie temperature window, which leads to a large ΔM and be in favor of the magnetic-field-induced structural transformation (MFIST). Based on this improvement, large MCE, reduced hysteresis loss (HL), and improved RC_{eff} are obtained.

*Project supported by the National Natural Science Foundation of China (Grant Nos. 51601092, 51571121, and 11604148), the Fundamental Research Funds for the Central Universities, China (Grant Nos. 30916011344 and 30916011345), Jiangsu Natural Science Foundation for Distinguished Young Scholars, China (Grant No. BK20140035), China Postdoctoral Science Foundation (Grant No. 2016M591851), the Natural Science Foundation of Jiangsu Province, China (Grant Nos. BK20160833 and BK20160829), Qing Lan Project of Jiangsu Province, China, Priority Academic Program Development of Jiangsu Higher Education Institutions, China, and NMG–NJUST Joint Scholarship Program for Ishfaq Ahmad Shah (Student ID: 914116020118).

†Corresponding author. E-mail: xufeng@njust.edu.cn

© 2017 Chinese Physical Society and IOP Publishing Ltd

2. Experimental details

The polycrystalline $Ni_{48-x}Co_2Mn_{38+x}Sn_{12}$ ($x = 0$, 1.0, 1.5, 2.0, and 2.5) alloys were prepared by arc-melting appropriate amounts of high purity elements Ni (99.995 wt.% purity), Co (99.95 wt.% purity), Mn (99.998 wt.% purity), and Sn (99.99 wt.% purity) in argon atmosphere. The samples were re-melted three times for homogeneity. The obtained ingots were annealed at 900 °C in vacuum for 24 h, and then quenched into cold water. The martensitic and reverse transformation behaviors were identified by differential scanning calorimetry (DSC) with the heating/cooling rate of 10 K/min. The crystal structures were investigated by powder x-ray diffraction (XRD) using Cu-K_α radiation at RT. The compositions of the elaborated alloys were confirmed by x-ray energy dispersive spectrometry (EDS). Magnetic measurements were performed on a physical property measurement system (PPMS). Isothermal magnetization (M–B) curves were measured using a so-called loop process to avoid the irreversibility caused by the magnetic-field-induced first-order MST.[23] Before each M–B measurement, the samples were cooled down to full martensitic state, and then gradually heated to the measurement temperature with a ramp rate of 3 K/min. To ensure the temperature stability of the measurement, a waiting time of 3 min was hold at the target temperatures.

3. Results and discussion

The XRD patterns of all the samples are shown in Fig. 1. For $x = 0$, the XRD pattern demonstrates a 4O modulated martensitic structure at RT. It suggests that the structural transformation in $Ni_{48}Co_2Mn_{38}Sn_{12}$ occurs above RT. While for $x = 2.5$, the presence of (111), (220), (400), and (422) peaks indicates a $L2_1$ austenitic structure with the lattice constant of $a = 5.978$ Å. The coexistence of austenitic and martenitic phases is observed in the samples with $0 < x < 2.5$ at RT. The XRD data indicates that T_t decreases with x increasing.[24]

The thermal-induced structural transformation was investigated by DSC measurements. As shown in Fig. 2, the large endothermic and exothermic peaks in the heating/cooling processes and the large thermal hysteresis indicate the occurrence of first-order structural transformation between martensite and austenite in these Heusler-type $Ni_{48-x}Co_2Mn_{38+x}Sn_{12}$ ($x = 0$, 1.0, 1.5, 2.0, and 2.5) alloys. As x increases from 0 to 2.5, the T_t shifts to the lower temperatures by around 85 K and 110 K in the heating and cooling processes, respectively. It is known that the T_t of Ni–Mn-based shape memory alloys is sensitive to the electron concentration (e/a), and it decreases with the e/a decreasing.[25–28] The e/a calculated from the EDS results for our samples are listed in Table 1. It can be found that with the increase of x, the e/a decreases from 8.115 to 8.025, resulting in the observed decrease of T_t.

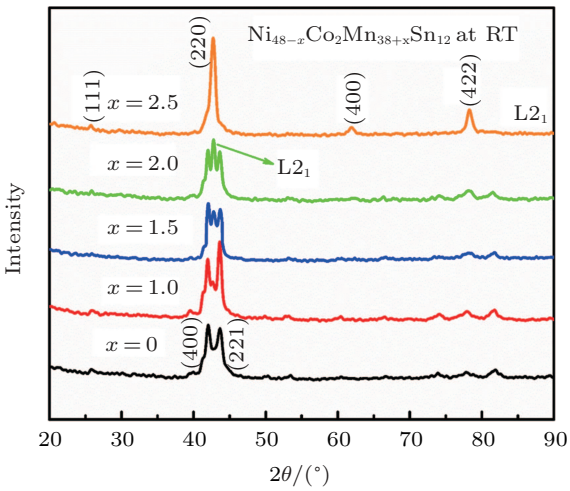


Fig. 1. (color online) Powder XRD patterns of $Ni_{48-x}Co_2Mn_{38+x}Sn_{12}$ ($x = 0$, 1.0, 1.5, 2.0, and 2.5) alloys at RT.

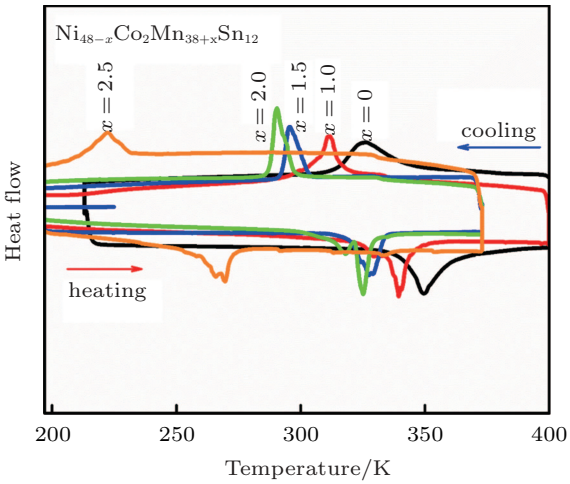


Fig. 2. (color online) DSC curves for $Ni_{48-x}Co_2Mn_{38+x}Sn_{12}$ ($x = 0$, 1.0, 1.5, 2.0, and 2.5) alloys in heating and cooling processes.

Table 1. The measured compositions and the characteristic phase-transition temperatures of $Ni_{48-x}Co_2Mn_{38+x}Sn_{12}$ ($x = 0$, 1.0, 1.5, 2.0, and 2.5) alloys.

x	Ni/at.%	Co/at.%	Mn/at.%	Sn/at.%	A_s/K	A_f/K	M_s/K	M_f/K	e/a
0	48.13	1.69	38.08	12.10	343	358	343	315	8.115
1.0	46.50	2.17	39.32	12.01	325	342	315	302	8.079
1.5	45.40	2.34	40.95	11.31	315	334	302	294	8.069
2.0	45.57	2.14	40.26	12.03	304	325	297	287	8.049
2.5	45.15	2.05	40.46	12.34	251	278	225	213	8.025

Figure 3 shows the temperature dependence of magnetization (M–T) of $Ni_{48-x}Co_2Mn_{38+x}Sn_{12}$ ($x = 1.0$, 1.5, 2.0, and 2.5) alloys under an applied field of 0.01 T during the heating and cooling processes. For $x = 1.0$, due to the fact of that the T_t in the heating process is close to the Curie-temperature of austenite ($T_{C,A} \approx 340$ K), the ferromagnetic austenite is not obviously observed in the heating process, but can be found in the cooling process. The existence of thermal hysteresis proves the first-order nature of the structural transformation between martensite and austenite. With x increasing from 1.5 to 2.5, the T_t shifts to the lower temperatures. As a result, the ferromagnetic austenite appears both in the heating and cooling processes. It is found that $T_{C,A}$ is nearly stable with the alteration of composition. The Curie temperature of martensite ($T_{C,M}$) is not observed in the samples with $x = 1.0$, 1.5, and 2.0 in the temperature range of 250–400 K, but is found in the $x = 2.5$ sample. In the heating process, the sample with $x = 2.5$ experiences the magnetic ordering-disordering transition of martensite, and then the first-order MST from the low-magnetization martensite to ferromagnetic austenite. The $T_{C,M}$ of $x = 2.5$ is around 208 K. A phase diagram including austenitic start temperature A_s, austenitic finish temperature A_f, martensitic start temperature M_s, martensitic finish temperature M_f, $T_{C,M}$, and $T_{C,A}$ for $Ni_{48-x}Co_2Mn_{38+x}Sn_{12}$ ($x = 0$, 1.0, 1.5, 2.0, and 2.5) alloys is shown in Fig. 4(a). According to Fig. 4(a), it can be found that with the increase of x, the T_t is decreased into the temperature window between $T_{C,A}$ and $T_{C,M}$. Thus, the samples with $x = 1.5$ and 2.0 exhibit the room-temperature MST between the weak-magnetization martensite and ferromagnetic austenite. This transition is accompanied by a large ΔM, which is favor of MFIST. Due to the existence of ΔM between martensite and austenite, the MST can be induced by a magnetic field. The M–B curves for $Ni_{48-x}Co_2Mn_{38+x}Sn_{12}$ ($x = 1.0$, 1.5, and 2.0) alloys with a temperature interval of 3 K in the heating process are shown in Figs. 4(b)–4(d). With the increase of the magnetic field, an obvious slope change is observed when the temperature is close to A_s. This behavior suggests the existence of MFIST from the martensite to austenite.[29–31]

According to the M–B curves, the MCE of $Ni_{48-x}Co_2Mn_{38+x}Sn_{12}$ ($x = 1.0$, 1.5 and 2.0) alloys is estimated by the Maxwell equation[32]

$$\begin{aligned}\Delta S_M(T,B) &= S_M(T,B) - S_M(T,0) \\ &= \int_0^B \left(\frac{\partial M(B,T)}{\partial T}\right)_B \mathrm{d}B. \end{aligned} \tag{1}$$

As shown in Fig. 5, the maximum values of magnetic entropy change (ΔS_M) with the magnetic field variation of 0–5 T are 19.22 J·kg^{-1}·K^{-1}, 13.64 J·kg^{-1}·K^{-1}, and 7.71 J·kg^{-1}·K^{-1} for $x = 1.0$, 1.5 and 2.0, respectively, and with the magnetic field variation of 0–2 T, the corresponding values decrease to 5.75 J·kg^{-1}·K^{-1}, 5.54 J·kg^{-1}·K^{-1}, and 3.57 J·kg^{-1}·K^{-1}, respectively.[33–38] The maximum ΔS_M decreases with the increase of x. It is found that the ΔS_M is inversely proportional to the transformation width (W), which gradually increases

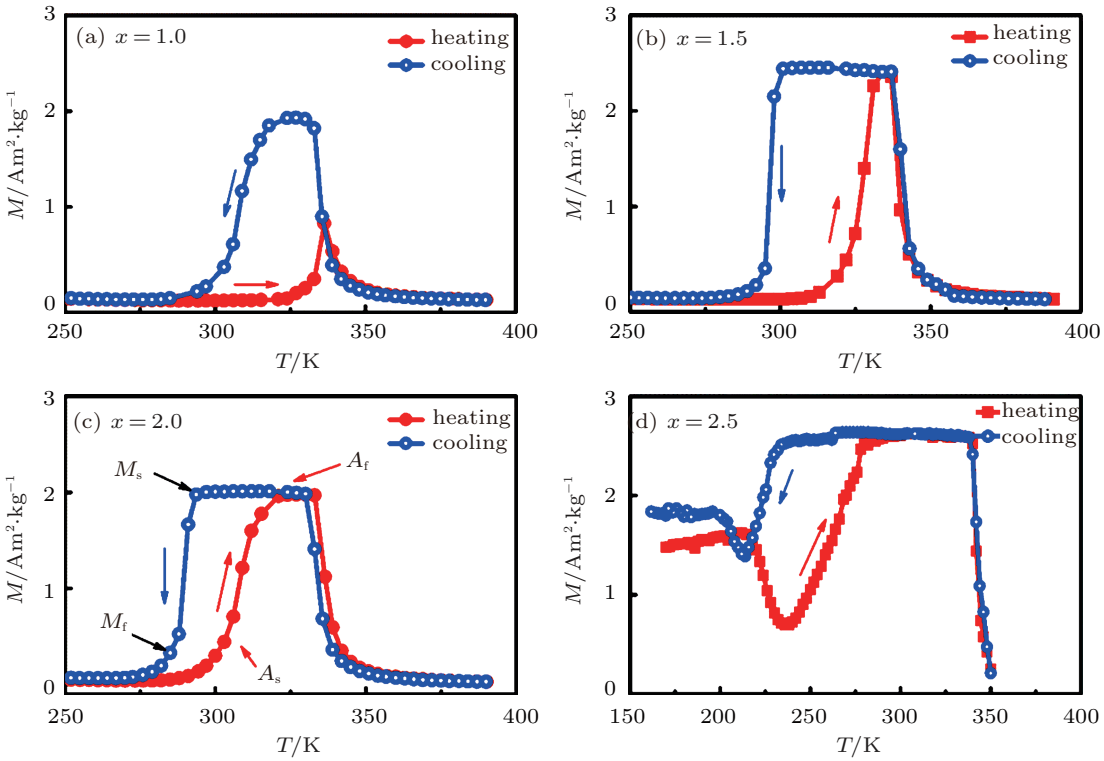


Fig. 3. (color online) M–T curves for $Ni_{48-x}Co_2Mn_{38+x}Sn_{12}$ ($x = 1.0$, 1.5, 2.0, and 2.5) alloys under an applied magnetic field of 0.01 T during the heating and cooling processes.

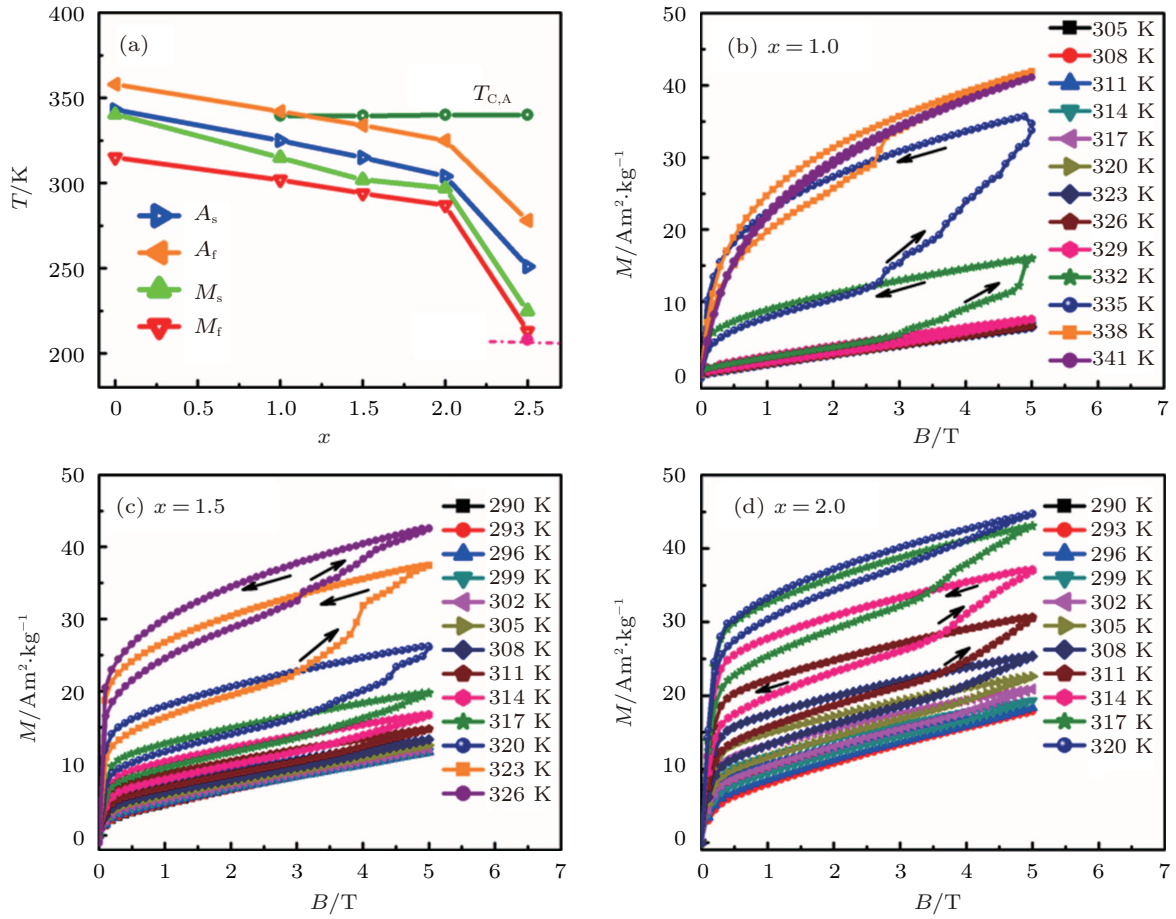


Fig. 4. (color online) (a) Phase diagram for $Ni_{48-x}Co_2Mn_{38+x}Sn_{12}$ ($x = 0$, 1.0, 1.5, 2.0, and 2.5) alloys as a function of x. (b)-(d) $M - B$ curves for $Ni_{48-x}Co_2Mn_{38+x}Sn_{12}$ ($x = 1.0$, 1.5, and 2.0) alloys with a maximum magnetic field of 5 T.

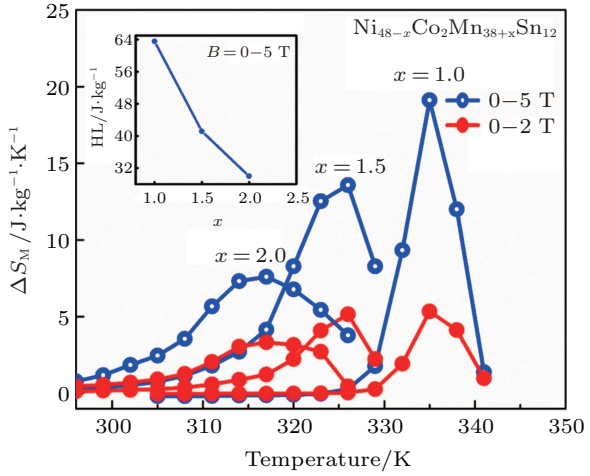


Fig. 5. (color online) Temperature dependence of magnetic entropy change for $Ni_{48-x}Co_2Mn_{38+x}Sn_{12}$ ($x = 1.0$, 1.5, and 2.0) alloys under the magnetic field variations of 0–2 and 0–5 T. The inset shows the x dependence of average HL for $Ni_{48-x}Co_2Mn_{38+x}Sn_{12}$ ($x = 1.0$, 1.5 and 2.0) alloys under a magnetic field variation of 0–5 T.

with x increasing (shown in Table 2). As mentioned by Cugini *et al.*,[39] the transformation width is highly related to the structural discontinuity between the martensite and austenite phases, impurities, vacancies, and interstitial defects in Heusler-type alloys. Wu *et al.*[40] also reported that the magnetostructural transformation in the Mn–Ni–Ge alloy becomes broadened when the grain size decreases. Therefore, there are various factors that can influence the transformation width. In this work, it is found that accompanied by the increase of x, the transformation width increases. So, the observed broadened transformation width may be related to the increased chemical disorder. Besides ΔS_M, the effective refrigeration capacity (RC_{eff}) is also an important parameter to evaluate the magnetic cooling capacity of MCE materials. Here, RC_{eff} is calculated by

$$RC_{eff} = \int_{T_{cold}}^{T_{hot}} \Delta S_M \, dT - \text{average HL}, \tag{2}$$

where T_{cold} and T_{hot} are the temperatures corresponding to the full width at half maximum (FWHM) of the ΔS_M peak, and average HL is calculated from the area surrounded by the hysteresis loops (M–B curves in Fig. 4), as shown in the inset of Fig. 5.[41,42] The calculated values for the transformation width, T_{cold}, T_{hot}, ΔS_M, average HL, and RC_{eff} of $Ni_{48-x}Co_2Mn_{38+x}Sn_{12}$ alloys are summarized in Table 2. Although the maximum ΔS_M decreases with x increasing, the average HL is remarkably reduced. Therefore, an enhanced RC_{eff} is obtained in the samples with $x = 1.5$ and 2. The calculated values of RC_{eff} are 23.36 J·kg^{-1},

60.79 J·kg^{-1}, and 67.60 J·kg^{-1} for $x = 1.0$, 1.5, and 2.0 with the magnetic field variation of 0–5 T, respectively, which are comparable to those of some other Ni–Mn-based Heusler alloys, such as $Ni_{42}Co_8Mn_{30}Fe_2Ga_{18}$ (70 J·kg^{-1}, $\Delta B = 5$ T), $Ni_{42.8}Mn_{40.3}Co_{5.7}Sn_{11.2}$ (72.10 J·kg^{-1}, $\Delta B = 3$ T), $Ni_2Mn_{0.75}Cu_{0.25}Ga$ (72 J·kg^{-1}, $\Delta B = 5$ T), $Ni_{50}Mn_{37}Sn_{13}$ (54 J·kg^{-1}, $\Delta B = 5$ T), $Ni_{45}Co_5Mn_{38}Sb_9Ge_3$ (54 J·kg^{-1}, $\Delta B = 5$ T), and $Ni_{52}Mn_{26}Ga_{22}$ (58.7 J·kg^{-1}, $\Delta B = 5$ T).[43–48]

Table 2. The transformation width $W(=A_f - A_s)$, T_{cold}, T_{hot}, magnetic entropy change ΔS_M, hysteresis loss (HL), and effective refrigeration capacity (RC_{eff}) of $Ni_{48-x}Co_2Mn_{38+x}Sn_{12}$ (x=1.0, 1.5, and 2.0) alloys.

x	W/K	T_{cold}/K	T_{hot}/K	$\Delta S_M(\Delta B = 5$ T) /J·kg^{-1}·K^{-1}	HL/J·kg^{-1}	RC_{eff}/J·kg^{-1}
1.0	17	332	338	19.22	63.13	23.36
1.5	19	319	329	13.64	41.51	60.79
2.0	21	308	225	7.71	30.70	67.60

4. Conclusion

In summary, we investigate the structural transformation and MCE in $Ni_{48-x}Co_2Mn_{38+x}Sn_{12}$ alloys with $x = 0$, 1.0, 1.5, 2.0, and 2.5. The partial substitution of Ni by Mn stabilizes the austenite phase and leads to the decrease of T_t. For the samples with $x = 1.5$ and 2, the MST between the weak-magnetization martensite and ferromagnetic austenite is achieved at RT. This transition is accompanied by a large ΔM, which is favor of MFIST. Accompanied by the MFIST, a considerable MCE is obtained. Maximum values of ΔS_M are 19.22 J·kg^{-1}·K^{-1}, 13.64 J·kg^{-1}·K^{-1}, and 7.71 J·kg^{-1}·K^{-1} for $x = 1.0$, 1.5, and 2.0 under the magnetic field variation of 0–5 T, respectively. Although the maximum ΔS_M is reduced with x increasing, the RC_{eff} is remarkably improved.

References

[1] Gutfleisch O, Willard M A, Bruck E, Chen C H, Sankar S G and Liu J P 2011 *Adv. Mater.* **23** 821
[2] Guillou F, Porcari G, Yibole H, Van Dijk N and Bruck E 2014 *Adv. Mater.* **26** 2671
[3] Lyubina J 2017 *J. Phys. D: Appl. Phys.* **50** 053002
[4] Shah I A, Hassan N, Liu J, Gong Y Y, Zhou X G and Feng X 2017 *Chin. Phys. B* **26** 017501
[5] Liu J, Gottschall T, Skokov K P, Moore J D and Gutfleisch O 2012 *Nat. Mater.* **11** 620
[6] Wada H, and Tanabe Y 2001 *Appl. Phys. Lett.* **79** 3302
[7] Hu F, Shen B, Sun J, Wang G and Cheng Z 2002 *Appl. Phys. Lett.* **80** 826
[8] Tagus O, Bruck E, Buschow K and Boer F D 2002 *Nature* **415** 150
[9] Han Z D, Wang D H, Qian B, Feng J F, Jiang X F and Du Y W 2010 *J. Appl. Phys.* **49** 010211
[10] Zhang Y, Liu J, Zheng Q, Zhang J, Xia W, Du J and Ya A 2014 *Scr. Mater* **75** 26
[11] Quetz A, Koshkidko Y S, Titov I, Rodionov I, Pandey S, Aryal A, Ibarra-Gaytan P J, Prudnikov V, Granovsky A, Dubenko I, Samanta T, Cwik J, Llamazares J L S, Stadler S, Lahderanta E and Ali N 2016 *J. Alloys Compd.* **683** 139
[12] Xuan H C, Han P D, Wang D H and Du Y W 2014 *J. Alloys Compd.* **582** 369
[13] Varzaneh A G, Kameli P, Karimzadeh F, Aslibeiki B, Varvaro G and Salamati H 2014 *J. Alloys Compd.* **598** 6
[14] Li Z, Xu K, Zhang Y L and Jing C 2015 *J. Appl. Phys.* **117** 023902
[15] Ma S C, Shih C W, Liu J, Yuan J H, Lee S Y, Lee Y I, Chang H W and Chang W C 2015 *Acta Mater.* **90** 292
[16] Xuan H C, Zheng Y X, Ma S C, Cao Q Q, Wang D H and Du Y W 2010 *J. Appl. Phys.* **108** 103920
[17] Chen F H, Huang Q X, Jiang Z Y, Xuan H C, Zhang M G, Xu X H and Zhao J W 2016 *Smart Mater. Struct.* **25** 6
[18] Zheng H, Wang W, Xue S, Zhai Q, Frenzel J and Luo Z 2013 *Acta Mater* **61** 4648
[19] Huang L, Cong D Y, Suo H L and Wang Y D 2014 *Appl. Phys. Lett.* **104** 132407
[20] Ma S C, Wang D H, Zhong Z C, Luo J M, Xu J L and Du Y W 2013 *Appl. Phys. Lett.* **102** 032407
[21] Moya X, Narayan S K and Mathur N D 2014 *Nat. Mater.* **13** 439
[22] Chen F, Tong Y X, Tian B, Li L, Zheng Y F and Liu Y 2013 *J. Magn. Magn. Mater.* **347** 72
[23] Caron L, Ou Z Q, Nguyen T T, Cam-Thanh D T, Tegus O and Bruck E 2009 *J. Magn. Magn. Mater.* **321** 3559
[24] Maziarz W, Czaja P, Szczerba M J, Dobrzynska L L, Czeppe T and Dutkiewicz J 2014 *J. Alloys Compd.* **615** S173
[25] Cong D Y, Roth S and Schultz L 2012 *Acta Mater.* **60** 5335
[26] Srivastava V, Chen X and James R D 2010 *Appl. Phys. Lett.* **97** 014101
[27] Bhatti K P, Khatib S E, Srivastava V, James R D and Leighton C 2012 *Phys. Rev. B* **85** 134450
[28] Chen F H, Gong C W, Guo Y P, Zhang M G and Chai Y S 2013 *Phys. Status Solidi A* **210** 2762
[29] Emre B, Bruno N M, Emre S Y and Karaman I 2014 *Appl. Phys. Lett.* **105** 231910
[30] Luo H, Meng F, Jiang Q, Liu H, Liu E, Wu G and Wang Y 2010 *Scr. Mater.* **63** 569
[31] Ye M, Kimura A, Miura Y, Shirai M, Cui Y T, Shimada K, Namatame H, Taniguchi M, Ueda S, Kobayashi K, Kainuma R, Shishido T, Fukushima K and Kanomata T 2010 *Phys. Rev. Lett.* **104** 176401
[32] Zhong Z C, Ma S C, Wang D H and Du Y W 2012 *J. Mater. Sci. Technol.* **28** 193
[33] Pecharsky V K and Gschneidner Jr K A 1997 *Phys. Rev. Lett.* **78** 4494
[34] Benford S M and Brown G V 1981 *J. Appl. Phys.* **52** 2110
[35] Krenke T, Duman E, Acet M, Moya X, Manosa L and Planes A 2007 *J. Appl. Phys.* **102** 033903
[36] Sharma V K, Chattopadhyay M K and Roy S B 2010 *J. Phys. D: Appl. Phys.* **43** 225001
[37] Xuan H C, Chen F H, Han P D, Wang D H and Du Y W 2014 *Intermetallics* **47** 31
[38] Niemann R, Heczko O, Schultz L and Fahler S 2010 *Appl. Phys. Lett.* **97** 222507
[39] Cugini1 F, Porcari G, Fabbrici S, Albertini F and Solzi M 2016 *Phil. Trans. R. Soc. A* **374** 20150306
[40] Wu R, Shen F, Hu F, Wang J, Bao L, Zhang L, Liu Y, Zhao Y, Liang F, Zuo W, Sun J and Shen B 2016 *Sci. Rep.* **6** 20993
[41] Brock J and Khan M 2017 *J. Magn. Magn. Mater.* **425** 1
[42] Sharma V K, Chattopadhyay M K and Roy S B 2007 *J. Phys. D: Appl. Phys.* **40** 1869
[43] Pathak A K , Dubenko I, Karaca H E, Stadler S and Ali N 2010 *Appl. Phys. Lett.* **97** 062505
[44] Chen F H, Gong C W, Guo Y P, Zhang M G and Chai Y S 2014 *Chin. Phys. B* **23** 067501
[45] Stadler S, Khan M, Mitchell J, Ali N, Gomes A M, Dubenko I, Takeuchi A Y and Guimaraes A P 2006 *Appl. Phys. Lett.* **88** 192511
[46] Phan T L, Zhang P, Dan N H, Yen N H, Thanh P T, Thanh T D, Phan M H and Yu S C 2012 *Appl. Phys. Lett.* **101** 212403
[47] Sahoo R, Nayak A K, Suresh K G and Nigam A K, 2012 *J. Magn. Magn. Mater.* **324** 1267
[48] Li Z B, Zhang Y D, Sanchez-Valdes C F, Sanchez-Llamazares J F, Esling C, Zhao X and Zuo L 2014 *Appl. Phys. Lett.* **104** 044101